Microstructural evolution and nano-mechanical properties of Ti-Al-based alloys synthesized by laser in-situ alloying

L. R. Kanyane[a] , *A.P.I* Popoola[a], *S.* Pityana[b] and *M.* Tlotleng[b,c]
[a]*Department of Chemical, Metallurgical and Materials Engineering, Tshwane University of Technology, P.M.B. X680, Pretoria, South Africa*
[b]*Laser Materials Processing Group, National Laser Center CSIR, Pretoria 0001, South Africa*
[c]*Department of Mechanical Engineering Science, University of Johannesburg, Auckland Park Campus, Johannesburg, South Africa*
Correspondence: lrkanyane@gmail.com , MTlotleng@csir.co.za

Abstract. Developing titanium aluminides (Ti-Al) based alloys by means of Laser Engineered Net Shaping (LENS) in-situ manufacturing yields attractive properties as compared to other fabrication methods. Ti-Al alloys have attracted much attention for high-temperature performance in gas turbine and automobile applications because of their attractive properties such as low density, high strength, high stiffness, and good oxidation resistance. In this work, laser in-situ fabricated Ti-Al-2Cr (Sample C3), Ti-Al-3Cr (Sample C1) and Ti-Al-4Cr (Sample C2) alloys were developed and the compositional effect on morphological evolution and nano-mechanical properties were investigated. The developed alloys were heat treated to 1350^{o}C and air-cooled. The microstructural evolution was characterized using the scanning electron microscope (SEM) equipped with energy dispersive spectroscopy (EDS). Anton-Paar equipment was used to analyze the nanoindentation properties (hardness, elastic modulus and stiffness) and MatLab software was utilized to analyze the stress-strain behaviour of the alloys from the nanoindentation load-displacement curve. The results showed that normalizing heat-treatment played an important role in homogenizing the alloys and there was a significant decrease in nanoindentation hardness, stiffness and modulus of elasticity after heat-treatment.

1 Introduction

Titanium aluminides (Ti-Al) alloys centered on the γ-TiAl phase have presented numerous benefits such as low density, high specific strength, and excellent resistance against oxidation, creep, and corrosion [1]. For that reason, γ-TiAl alloys are favorable high-temperature structural materials in the aerospace engines field, such as compressor blades, turbine wheels, and pistons [2-5]. However, due to their poor ductility at room temperature, Ti-Al structural components are puzzling to manufacture [6-8]. The effect of well-known alloying elements which form the backbone of the ever-promising intermetallic titanium

aluminides has been an area of research to better understand how to best optimize the properties of the alloys by increasing the ductility for advanced engineering applications.
According to Liu [9], the benefits of alloying elements are (i) to cause relaxation of slip modes restriction; (ii) to reduce the ordering kinetics or alter long-range ordering degrees; (iii) to modify the alloy structure by introducing β-phase as a ductile phase to mitigate micro-crack formation in α2/γ phases; and (iv) to adjust transformation behaviour when processing or heat treating to facilitate the control of microstructural refinement. The addition of chromium (Cr) was noted to have a beneficial effect on the Ti-Al matrix [10, 11].
Laser additive manufacturing (LAM), also known as 3D printing, which achieves material printing by piling incremental melt pools of materials layer by layer offers a new path for the synthesizing of Ti-Al-based alloys and complex components [5, 12]. Here, additive manufacturing is known to be more economical than conventional methods. With direct metal laser deposition, the molten pool cools and solidifies rapidly producing metal parts of superior quality and strength with no material waste as compared to conventional machining [13-16]. It was found that the LAM process can reduce production time by 40% and lower labour and capital equipment costs. However, during LAM, high thermal stresses are experienced in the process due to the rapid cooling nature of the process which could lead to the developed alloys having high stress [17-19]. Heat treatment (HT) is regarded as the post-processing technique which can homogenize the microstructure of the as-built laser samples while relieving them of internal stress. According to the Ti-Al binary phase diagram different heat treatment temperatures and strategies can be used to produce different microstructures. This is dependent on the method of cooling and the aluminium content present in the alloy or composition [5, 7, 19, 20].

From the reviewed literature, it is evident that a major gap in knowledge exists in the in-situ development of Ti-Al-xCr alloys from pure metallic powders. There is limited or no information in scientific publications or studies that report the nano-indentation performance of Ti-Al-xCr alloys in addition to retaining improved stress-strain compressive properties. This work aims at synthesizing Ti-Al-xCr ternary alloys via laser in-situ alloying using 850-R Optomec Laser Engineered Net Shaping (LENS) machine and investigate the effects of normalizing heat treatment (HT) on the microstructure and nano-mechanical properties. Most importantly, this paper will for the first time report on the nanoindentation stress-strain behaviour of ternary γ-TiAlCr alloys coded via MatLab software following the load-displacement behaviour results.

2 Methodology

850-R Optomec LENS machine was used to manufacture Ti-Al test coupons. This manufacturing platform uses a 1000 W IPG fibre laser which is connected to the deposition head. The set-up allowed for the laser beam and depositing powder(s) to be concentric and controlled simultaneously during deposition. The set-up is controlled automatically, during 3D printing, from an overhead computer screen that is installed with the Workstation Control Software, version 3.1.10. A total number of three 3D printed in order to ascertain the preferred qualities of the built samples. For optimal LAM process parameters. Cr feed rate was randomized at different levels. The developed alloys were fabricated at the laser power of 450W with a scan speed of 26in/min. The feed rate of Ti and Al were 2 and 1.4rpm which translated to the powder feed rate of 2.21 and 0.48g/min, respectively. The Cr feed rate was set at 0.1rpm (sample C1), 0.2 rpm (sample C2) at 1L/min gas carrier and 0.1rpm (sample C3) at 2L/min Cr gas carrier. The center purge gas flow rate was at 25L/min with the gas

carrier of Ti and Al set to 4.1 and 2.4L/min respectively. The experimental protocol is coherent with the work of Kanyane *et.al* [12]

2.1 Heat treatment

In this work heat treatment was conducted using a Carbolite tube furnace in an argon-rich environment. The samples were heated to a temperature of 1350 °C, before being air cooled. The temperature was ramped at 20 °C/min from room to the set temperature and held for 1 hour before air cooling (see Table 1). Heat-treatment was performed in order to homogenize the phase distribution along the synthesized samples.

Table 1: Heat treatment conditions

Sample ID	Temperature (°C)	Holding time (min)	Method of cooling
HT	1350	60	Air cooling

2.2 Nano-Indentation and Microhardness

The nanoindentation results are obtained via Oliver and Pharr method extrapolated from the load-displacement curve using Anton-Paar equipment. The applied load was set to be 400mN with 3000mN/min as the loading and unloading rate. MatLab was used to interpret the stress-strain curves from the nanoindentation load-displacement data. Elastic modulus, stiffness and nano-hardness were presented. Vickers microhardness (HVN) measurements of the developed Ti-Al-based were tested by means of the Zwick/Roell Indentec (ZHVμ) microhardness tester machine (Zwick Roell AG, Ulm, Germany) microhardness tester. The indention load was set to be 500kgf along with the dwell time of 15 seconds. Ten random indentations were tested and the average value was reported.

3 Results and Discussion

3.1 Microstructural analysis

Figure 1 presents the morphological evolution of the in-situ fabricated Ti-Al-xCr samples after HT at 1350ºC while **Figure 2** presents an EDS map of the HT samples. All samples presented complete phase transformation which resulted in fully lamellar structures. Rounded shape porosities can be observed in all the synthesized alloys. According to Dilip, Zhang [21], un-melted powder particles are more likely to produced irregularly shaped porosity at low applied energy density, and a high energy density is responsible for rounded porosity, which was due to keyhole effects. The molten-pool flow, particularly the keyhole effect, play an important part in the formation of the defects in crystallography during LAM. The increase in α + β phases in the alloy is known to reduce the alloy's machinability. According to Sibisi, Arthur [22], most AM components necessitate post HT in order to obtain good mechanical properties. All samples (C1, C2 and C3) possess a good response to heat treatments. The large volume of β precipitates can be observed in sample C1 and C3. Along the lamellar boundaries, it is clear that there are faults present that could trigger grain boundary dislocations in alloy C1 and C2. In the study of Tlotleng [8], the authors pointed out that the gamma-TiAl alloys after HT of 1400ºC transform into ultra-fine lamellar α + β

microstructure which proved to have outstanding mechanical properties. The EDS map and EDS spectrum (Table 2) proves that the doped Cr in Ti-Al matrix was homogeneously distributed in the alloys.

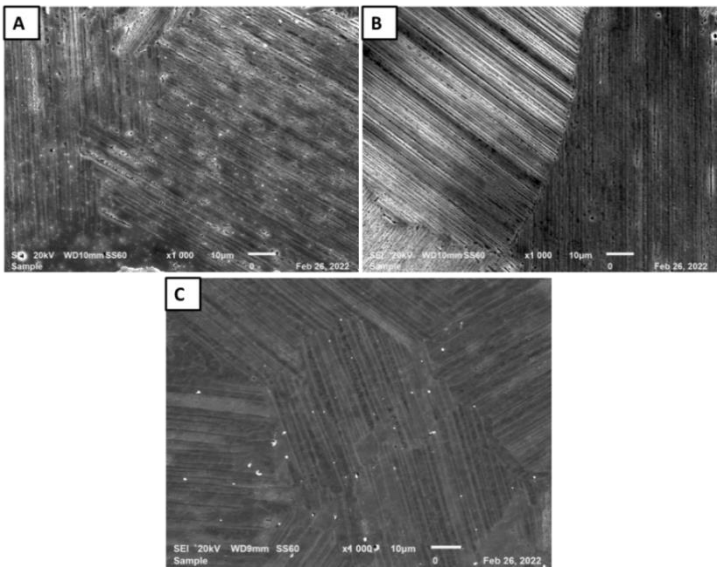

Figure 1: Morphological evolution of the in-situ fabricated samples after HT at 1350°C (a) C1, (b) C2 and (c) C3

Table 2: Elemental composition (at.%) of laser in-situ fabricated alloys after HT

Sample ID	Ti	Al	Cr
Ti-Al-3Cr (C1)	42.79 (43)	54.5 (55)	2.71 (3)
Ti-Al-4Cr (C2)	44.6 (45)	51.39 (51)	4.01 (4)
Ti-Al-2Cr (C3)	41.55 (42)	56.7 (57)	1.75 (2)

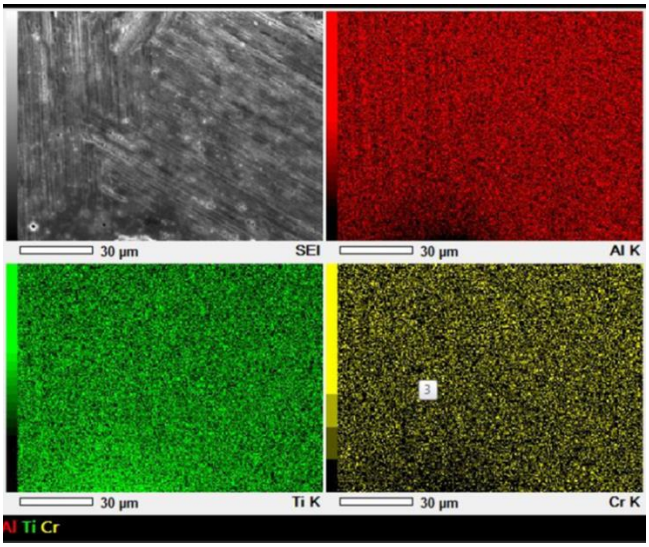

Figure 2: EDS map of the HT samples

3.2 Nanoindentation and Microhardness results

The nanoindentation tests conducted were used to examine the micro-mechanical properties of the synthesized TiAl-xCr alloys and the results are presented in Figure 3. From the developed samples, the hardness, elastic modulus and stiffness were recorded using a load-displacement curve using Anton-Paar equipment. The applied load was set to be 400mN. Nanoindentation gives the advantage to measure a material's properties on an extremely small scale [23]. From the results, it was observed that the incorporation of Cr had a greater effect on the mechanical properties of the synthesized Ti-Al matrix alloys. Modulus of elasticity (Er) show no significant trend for all the Ti-Al-Cr alloys, but it can be said that the bulk value show that the samples fall within the same Ti-Al family of material. The incorporation of Cr also leads to an increase in indentation hardness. However, after HT, there was a drastic decrease in hardness properties for samples C2 and C3. Maximum as-built hardness was evident in sample C2 with a value of 67384MPa. High stiffness properties were observed in all the samples with sample C2 high stiffness value of 1.1293mN/nm. All the in-situ developed samples have a significant decrease in stiffness value after HT.

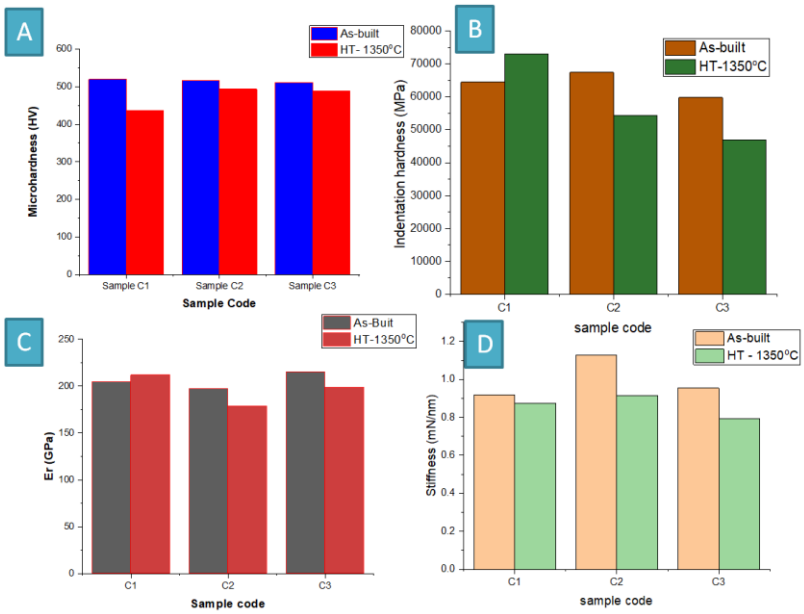

Figure 3: Effect of HT on mechanical properties of Ti-Al-xCr

3.3 Load-displacement results

The load-displacement curves of the in-situ synthesized Ti-Al-xCr alloys are presented in Figure 4. The results showed that the unloading retracts curve of samples C1 and C2 showed that there is a minimal permanent deformation in the two alloys while sample C3 shows no permanent distortion. There was a huge variation of the indentation force between samples C1, and C2 with sample C3 as presented, however, the resulted depth signified a minimal difference between the alloys. This suggests that the fabricated Ti-Al-xCr alloys are more resistant to plastic deformation. The microstructural results of the alloys show a fully lamellar structure with the presence of α2, γ along with β- structural phases. The β- phase is responsible for grain boundary pinning which resists the alloy from fully deformation under applied load. According to literature reports, plastic deformation for crystalline metals is attributed to the dislocation of slip. Remarkably, the combination of the phases in the developed alloy phase resulted in a reduction of the slipping plane which prevents interlunar dislocations. However, the HT microstructure presents grain boundary defects between the lamellar grains. Hence their indentation hardness was reduced proving that there was higher deformation taking place in the alloys.

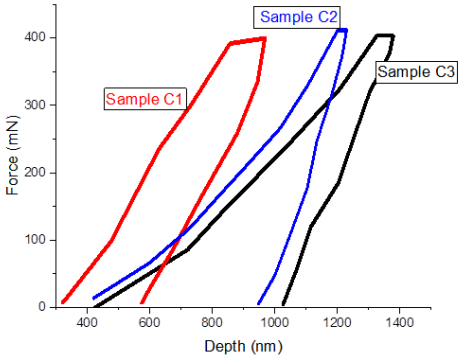

Figure 4: Load-displacement curve

3.4 Nanoindentation stress-strain

The stress-strain curve results were obtained by using a mathematical tool MatLab which was used to analyze and design the indentation process with a programming language that expresses matrix and array mathematics directly. The pyramid diamond indenter radii Birkovich tip was taken to be $15e^{-6}$nm (R) while the stiffness of the produced alloys varied between 0.78 - $1.15e^{6}$mN/nm (S). The following equations were used to calculate the stress-strain of the LENS developed titanium aluminides on MatLab software.

In the models, Oliver and Pharr [24] method was used to determine the compressive engineering stress-strain for the developed alloys. From the load-displacement curve, a relationship between contact pressure and contact strain during the elastic loading and unloading can be established as a linear relationship.

$P = a(h - hr)^m$ (Equation 1)

The equation above was recommended by Olive and Pharr to fit the nanoindentation load-displacement curve (*P*-*h*). *P* is the indentation load and *h* is the elastic displacement. From this equation, the elastic contact stiffness can easily be calculated from the upper portion of the *P*-*h* curve. During indentation, the relationship between indentation radii, R, contact radii, a and contact depth, hp can be deduced from:

$A = \sqrt{2hpR - hp^2}$ (Equation 2)

The above-mentioned equations can automatically calculate the stress-strain curve from the nanoindentation system which records the *P*-*h* response of the fabricated alloys. The engineering stress-strain response of the synthesized alloy was calculated from the following equations.

$\varepsilon = \frac{0.2a}{R}$ (Equation 3)

$\sigma = \frac{Pm}{3}$ (Equation 4)

The above-mentioned equations are appropriate descriptive of engineering stress-strain were ε *and* σ are strain and stress, respectively and where Pm is the contact pressure. Figure 5 present the stress-strain curves for Ti-Al-xCr in-situ developed samples. The results were obtained from a mathematical tool MatLab that was used to analyze and design the indentation process. The calculated stress-strain used follows Oliver and Pharr method. Sample C2 with Cr content of 4 at.% presented good ductility as compared to sample C1. It is clear that sample C1 (3 at.% Cr) showed high UTS as compared to sample C2. Both alloys showed good ductility behaviour at room temperature. The fabricated alloys are suitable for

engineering applications due to their Cr content of less than 10 a.t%. Both curves presented a pop-in effect due to the inhomogeneity of depth sensitive hardness properties of the fabricated alloys. These result in various dislocation nucleation movements during nanoindentation**.**

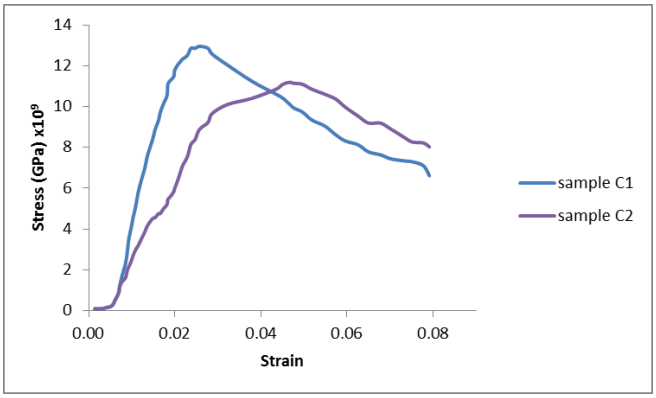

Figure 5: Nanoindentation stress-strain curves for sample C1 and C2

Conclusions

Ti-Al-xCr alloys were synthesized via in-situ alloying by means LENS technique. The influence of Cr on microstructural evolution and nano-mechanical behaviour of the developed Ti-Al-xCr alloys were investigated.

- SEM micrographs of the fabricated Ti-Al-Cr alloys, after HT, demonstrated no cracks, but only small rounded pores which are the result of the applied energy density leading to keyhole effect and EDS map analysis confirms the presence of the elements used to synthesize the Ti-Al-based alloys.
- The maximum average microhardness of 493.98HV was achieved at sample C1 (Ti-Al-3Cr) while the minimum HV value of 435.89HV was achieved at sample C3 (Ti-Al-2Cr) after HT at 1350^{o}C followed by air cooling.
- The nanoindentation stiffness of the as-built samples was high as compared to HT samples.

Acknowledgment

The authors would like to show their appreciation to the following organizations: Council of Scientific and Industrial Research (CSIR) along with Surface Engineering Research Centre (SERC), Tshwane University of Technology, Department of Chemical, Metallurgical and Materials Engineering, Pretoria, South Africa

References

1. Raji, S.A., A.P.I. Popoola, S.L. Pityana, and O.M. Popoola, *Characteristic effects of alloying elements on β solidifying titanium aluminides: A review.* Heliyon, 2020. **6**(7), e04463.
2. Weisheit, A., S.-K. Rittinghaus, A. Dutta, and J.D. Majumdar, *Studies on the effect of composition and pre-heating on microstructure and mechanical properties of direct laser clad titanium aluminide.* Optics and Lasers in Engineering, 2020. **131**, 106041.

3. Kumar, V.A., R. Gupta, M. Prasad, and S.N. Murty, *Recent advances in processing of titanium alloys and titanium aluminides for space applications: A review.* Journal of Materials Research, 2021, 1-28.
4. Neumeier, S., J. Bresler, C. Zenk, L. Haußmann, A. Stark, F. Pyczak, and M. Göken, *Partitioning Behavior of Nb, Ta, and Zr in Fully Lamellar γ/α2 Titanium Aluminides and Its Effect on the Lattice Misfit and Creep Behavior.* Advanced Engineering Materials, 2021, 2100156.
5. Kanyane, L.R., A.P. Popoola, S. Pityana, and M. Tlotleng, *Heat-treatment effect on anti-corrosion behaviour and tribological properties of LENS in-situ synthesized titanium aluminide.* International Journal of Lightweight Materials and Manufacture, 2022. **5**(2), 153-161.
6. Tlotleng, M., B. Masina, and S. Pityana, *Characteristics of laser In-situ alloyed titanium aluminides coatings.* Procedia Manufacturing, 2017. **7**, 39-45.
7. Seidel, A., S. Saha, T. Maiwald, J. Moritz, S. Polenz, A. Marquardt, J. Kaspar, T. Finaske, E. Lopez, and F. Brueckner, *Intrinsic Heat Treatment Within Additive Manufacturing of Gamma Titanium Aluminide Space Hardware.* JOM, 2019. **71**(4), 1513-1519.
8. Tlotleng, M., *Microstructural properties of heat-treated LENS in situ additively manufactured titanium aluminide.* Journal of Materials Engineering and Performance, 2019. **28**(2), 701-708.
9. Liu, Y., *Local Structure of Al-based Amorphous Alloys after Microalloying by Element Substitution and after Ball Milling.* 2012.
10. Panin, P., A. Kochetkov, A. Zavodov, and E. Lukina, *Effect of Gd addition on phase composition, structure, and properties of beta-solidifying TiAl-based alloy with Zr and Cr content variability.* Intermetallics, 2020. **121**, 106781.
11. Ye, L.-H., H. Wang, G. Zhou, Q.-M. Hu, and R. Yang, *Phase stability of TiAl-X (X= V, Nb, Ta, Cr, Mo, W, and Mn) alloys.* Journal of Alloys and Compounds, 2020. **819**, 153291.
12. Kanyane, L.R., A.P.I. Popoola, S. Pityana, and M. Tlotleng, *Synthesis of Ti-Al-xNb Ternary Alloys via Laser-Engineered Net Shaping for Biomedical Application: Densification, Electrochemical and Mechanical Properties Studies.* Materials, 2022. **15**(2), 544.
13. Reith, M., M. Franke, M. Schloffer, and C. Körner, *Processing 4th generation titanium aluminides via electron beam based additive manufacturing–characterization of microstructure and mechanical properties.* Materialia, 2020. **14**, 100902.
14. Wang, J., Q. Luo, H. Wang, Y. Wu, X. Cheng, and H. Tang, *Microstructure characteristics and failure mechanisms of Ti-48Al-2Nb-2Cr titanium aluminide intermetallic alloy fabricated by directed energy deposition technique.* Additive Manufacturing, 2020. **32**, 101007.
15. Lei, X., X. Wang, F. Kong, H. Zhou, and Y. Chen, *A moving-boundary dynamic model for in-situ alloyed and additive manufacturing TiAl-Nb alloys.* Journal of Manufacturing Processes, 2022. **73**, 563-571.
16. Zhang, C., Y. Liu, J. Lu, L. Xu, Y. Lin, P. Chen, Q. Sheng, and F. Chen, *Additive Manufacturing and Mechanical Properties of Martensite/Austenite Functionally Graded Materials by Laser Engineered Net Shaping.* Journal of Materials Research and Technology, 2022.
17. Tlotleng, M., T. Lengopeng, M.N. Seerane, and S.L. Pityana, *Effects of heat-treatment on the microstructure of TiAl-Nb produced with laser metal deposition technique.* 2017.

18. Agapovichev, A., A. Sotov, V. Kokareva, and V. Smelov. *Possibilities and limitations of titanium alloy additive manufacturing*. in *MATEC Web of Conferences*. 2018. EDP Sciences
19. Tlotleng, M. and S. Pityana, *Effects of Al and heat treatment on the microstructure and hardness of Ti–Al synthesized via in situ melting using LENS.* Metals, 2019. **9**(6), 623.
20. Kim, Y.-K., J.K. Hong, and K.-A. Lee, *Enhancing the creep resistance of electron beam melted gamma Ti–48Al–2Cr–2Nb alloy by using two-step heat treatment.* Intermetallics, 2020. **121**, 106771.
21. Dilip, J., S. Zhang, C. Teng, K. Zeng, C. Robinson, D. Pal, and B. Stucker, *Influence of processing parameters on the evolution of melt pool, porosity, and microstructures in Ti-6Al-4V alloy parts fabricated by selective laser melting.* Progress in Additive Manufacturing, 2017. **2**(3), 157-167.
22. Sibisi, P., N. Arthur, and S. Pityana, *Review on direct metal laser deposition manufacturing technology for the Ti-6Al-4V alloy*. The International Journal of Advanced Manufacturing Technology, 2020, 1-16.
23. Li, W., W. Yu, Q. Xu, J. Zhou, H. Nan, Y. Yin, and X. Shen, *Understanding the atomistic deformation mechanisms of polycrystalline γ-TiAl under nanoindentation: Effect of lamellar structure.* Journal of Alloys and Compounds, 2020. **828**, 154443.
24. Oliver, W.C. and G.M. Pharr, *An improved technique for determining hardness and elastic modulus using load and displacement sensing indentation experiments.* Journal of materials research, 1992. **7**(6), 1564-1583.